CONSTITUTIVE MODEL DEVELOPMENT AND RESIDUAL STRESS ANALYSIS FOR AM HASTELLOY X

Bachelor Thesis

Robert Lengwiler
15-918-972

January 20, 2020

Supervisor: Eduardo Mazza
Co-Supervisor: Ehsan Hosseini
Experimental Continuum Mechanics, EMPA

Contents

Abstract

Stress-strain response measured from tensile-compressive loading of Hastelloy X at a variety of temperatures are used to derive kinematic hardening model parameters, both with and without isotropic hardening as well as creep parameters. Isotropic hardening turn out to be of little consequence. These parameters are used to simulate an SLM process in ABAQUS in order to derive residual stresses and the resulting deformations. We were able to confirm the theory that describes the origin of residual stresses occur in additive manufacturing, and pinpoint location of stress concentrations.

1. Aim of this thesis

Additive manufacturing is gaining importance in industry, especially in applications demanding high-performance and low weight. Examples are turbine blades or medicinal implants. However, this process can only be a viable alternative if its properties can be accurately predicted. As a result, accurate models predicting residual stresses and deformation are needed. Because those of additively manufactured pieces are different to other production processes, it needs its own set of testing.

The goal of this report is to adapt constitutive material models to the SLM-Process and compare how strongly the choice of model influences the stresses and deformation in the final part. We will use ABAQUS to both derive the model parameters and simulate the SLM Process.

2. Theory

2.1   Thermal origin of residual stresses

Selective laser melting (SLM) is an additive manufacturing process which uses a laser to melt metal powder, causing it to bind to its surroundings. This process can cause residual stresses to develop. The process by which this occurs is as follows:[1]

1. The heated metal will expand much more than the solid below it.

2. At high temperatures a material possesses a much lower yield point. Combined with a lack of obstruction this results in plastic deformation of the top layer. The ones below may experience compressive stresses.

3. As the metal cools it will shrink but is inhibited from doing so due to the substrate below.

4. This causes compressive stress in the substrate and tensile stress in the newest layer.

The effect is more pronounced, the larger the temperature gradient from layer to layer is, as this increases the difference of plastic deformation.[2] Therefore, the choice of constitutive model will predict different stresses and deformations. To what extent they vary is the goal of this thesis.

2.2   Definitions and general concepts

The deformation of a material can be separated into three main components: the elastic strain ε_e, the plastic strain ε_p, and the creep strain ε_{creep}. Elastic strain occurs if any load is applied and is best approximated using Hook's Law.

In order to describe plastic strain, three things are required: First: the point where the strain becomes plastic, which is described using the flow criterion f. [3]

Second: what is the stress-strain relation in the plastic region, which is derived using a flow rule. Third: how does the flow criterion change depending on the amount of plastic strain, which is described by selecting a hardening model.

The flow criterion f is equal to 0 if the strain is plastic and smaller than 0 if it is elastic. One of the most common description of the flow criterion is the Mises criterion(see Figure 2.1) :

$$f = \sqrt{\frac{3}{2}\underline{S} : \underline{S}} - \sigma_y,$$

where S is the deviatoric stress and σ_y the initial yield stress. Definition of deviatoric stress: $\underline{S} = \underline{\sigma} - \frac{1}{3}(\underline{\sigma} \cdot \underline{I})\underline{I} = \underline{\sigma} - \underline{\sigma}_{Hydro}$.

Figure 2.1: 2D representation of the Mises yield criterion (blue: von Mises, black: tresca)

Once the stress state reaches the yield curve, it will change shape and/or move position. This is described using a hardening model, a selection of which is described in section 2.3.

The associated flow rule (sometimes referred to as normality rule) defines the plastic strain rate as:

$$d\dot{\varepsilon}_{pl} = d\dot{\lambda}\frac{df}{d\sigma}$$

where $d\dot{\lambda}$ is the plastic multiplier. Other flow rules have been postulated by Levy , Prantel and Reuss [4], but they are not considered here.

2.3 Constitutive Models

Constitutive models describe a relation between stress and strain. Of interest are especially the plastic deformation models. What follows is an overview over a selection of them and an explanation of some related basic concepts.

2.3.1 Elastic

Most materials exhibit rate-independent elastic(reversible) deformation at low deformation. In this region, Hook's Law describes the stress-strain relation best. In a

3-dimensional loading it is written as follows [3],

$$\underline{\varepsilon}^e = \frac{1+\nu}{E}[\underline{\sigma} - \frac{\nu}{1+\nu}(\underline{\sigma} \cdot \underline{I})\underline{I}] \qquad (2.1)$$

Since there is no plastic deformation, we do not have to concern ourselves with any flow condition or any hardening law. ABAQUS uses the same formula.

2.3.2 Elastic-Ideal-Plastic

The simplest plastic assumption is that once the yield point has been reached, the material deforms plastically without any hardening. The flow condition can be described by $f = \sqrt{\frac{3}{2}\underline{S}:\underline{S}} - \sigma_y(p)$. Because σ_0 remains constant the yield curve does not change. Very few metals exhibit this behaviour.

2.3.3 Elastic-Isotropic-hardening-Plastic

When a material hardens isotopically its yield surface expands proportionally in all directions when yield stress is exceeded, as seen in Figure 2.2. [4] Mathematically, isotropic hardening is represented as flows [5],

Flow Condition : $\quad f = \sqrt{\frac{3}{2}\underline{S}:\underline{S}} - \sigma_y(p)$
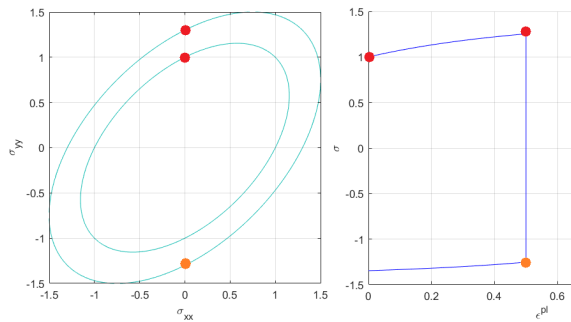
Figure 2.2: Isotropic Hardening

where p is the equivalent accumulated plastic strain. A purely isotropic model is suited for monotonic loading but not for cyclical loadings, as it is unable to model the Bauschinger effect.

2.3.4 Elastic-Kinematic-hardening-Plastic

A material that hardens kinematically has its flow condition centred around a backstress tensor α. [4] The evolution of the backstress tensor $\dot{\alpha}$ can therefore describe the hardening using the associated flow rule. This means that if the stress direction were to reverse, the yield strength would be different than if it had not (see Fig.2.3). This is commonly referred to as
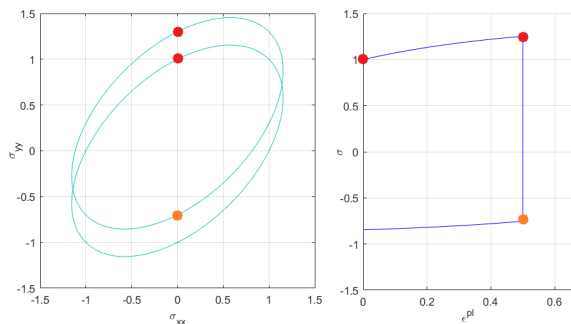
Figure 2.3: Kinematic Hardening

4

the Bauschinger effect, which is observed in most polycrystalline metals. Mathematically this Model can be described as follows:[6]

Flow Condition : $\qquad f = \sqrt{\dfrac{3}{2}(\underline{S} - \underline{\alpha}) : (\underline{S} - \underline{\alpha})} - \sigma_y(p)$

$\sigma_y = \sigma_0$ signifies pure kinematic hardening, while $\sigma_y = \sigma_y(p)$ signifies isotropic/kinematic hardening

Chaboche model

The Chaboche model is widely accepted and has been implemented into many FEM programs. [7] It too, assumes that the yield surface is centred around a backstress tensor α. As a result, the yield surface is written as,

$$f = \sqrt{\frac{3}{2}(\underline{S} - \underline{\alpha}) : (\underline{S} - \underline{\alpha})} - \underline{\sigma_y} - R(p)$$

where R is the isotropic part. For pure kinematic hardening $R = 0$. [8]

Chaboche's model allows for multiple backstress tensors. The evolution of the backstress tensor is thus written as

$$\underline{\alpha} = \sum_{i=1}^{m} \underline{\alpha}_i$$

with

$$d\underline{\alpha}_i = \frac{2}{3} C_i d\underline{\varepsilon}_{pl} - \gamma_i \underline{\alpha}_i |d\varepsilon_{pl}| + \frac{1}{C_i} \frac{dC_i}{dT} \underline{\alpha}_i dT \qquad (2.2)$$

where C_i and γ_i are temperature dependent material parameters, and m is equal to the number of backstress terms. In our case we will use 2.

A purely kinematic hardening model can explain certain phenomena like the Bauschinger effect (the yield stress is lower if the loading is reversed).

2.3.5 Creep and Relaxation
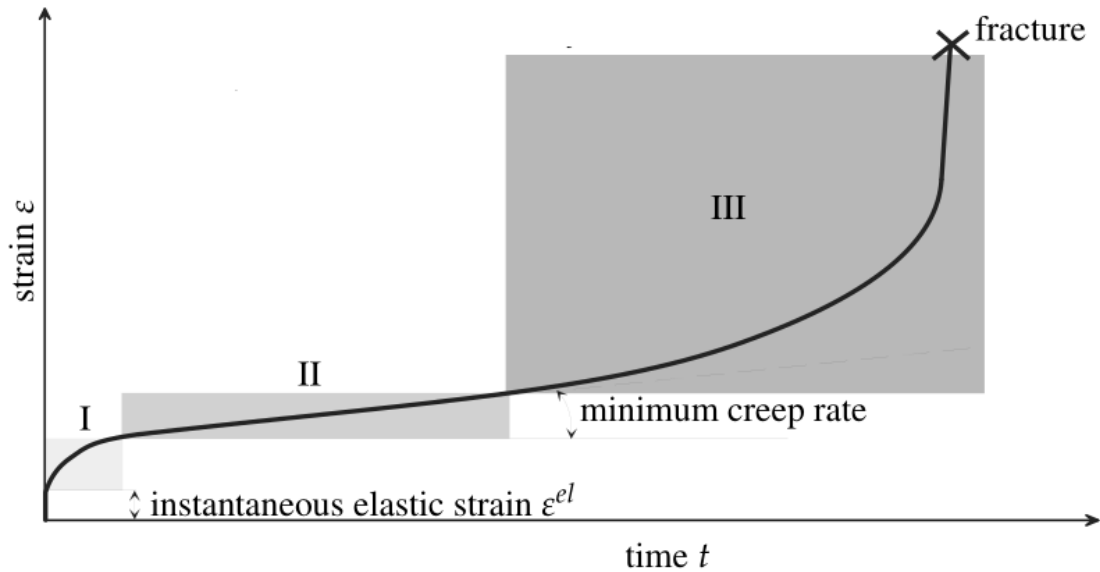
Figure 2.4: Creep Regions (picture taken from [9])

At elevated temperatures ($T > 0.3T_m$ for metals), a material under stress can deform plastically over time, despite being below the yield stress. This is referred to as creep which "is characterized by a variety of microstructural rearrangements". [9] Therefore, if the stress is held at a constant value, the deformation will continue to increase, which is referred to as creep. If the deformation is held constant, the stresses will decrease, which is referred to as relaxation. The strain can be separated into three different sections, referred to as creep regions, as pictured in Figure 2.4 [9]: In the primary region, referred to as transient creep, the strain rate decreases monotonic and within a short period of time. Mathematically, the strain in this region is commonly represented with the Norton-Bailey Law, or sometimes refered to as power-law: $\bar{\dot{\varepsilon}}_{cr} = A \cdot \bar{\sigma}^n t^m$. [10]

In the secondary region, referred to as steady creep, the strain rate is constant. It is also the most relevant for long-term descriptions of a part under stress, because it covers the largest time frame. Mathematically it can be represented using the Norton-Law: $\bar{\dot{\varepsilon}}_{cr} = A \cdot \bar{\sigma}^n t$.

In the tertiary region, referred to as accelerating creep, the strain rate increases exponentially until failure, due to microscopic fractures within the grain boundaries. [9] While models for this region exist, they are not relevant for this thesis and will not be discussed.

For our simulation we will use the Norton-Law, despite the hold time being relatively short. The reason for this is, that neither law is suitable for cyclical loading. [10] As such, we need to commit to a simplified model if we want to model creep at all.

3. Measurements

Mechanical tests of Hastelloy X have been performed by E. Hosseini at $25°C$, $200°C$, $400°C$, $600°C$, $800°C$. The measuring apparatus is pictured in figure 3.1. The specimen is subjected to a series of deformation patterns. They consist of up to seven segments: four ramp cycles and three hold cycles. During the ramp, the specimen is deformed to 0.75% with a variety of deformation rates ($0.001s^{-1}, 0.0002s^{-1}$ and $0.005s^{-1}$) which is be followed by a hold time of 15min, as well as one series with a deformation rate of $0.001s^{-1}$ without hold time.
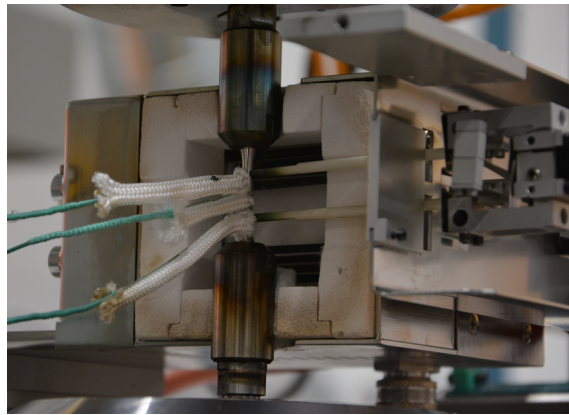
Figure 3.1: Measuring apparaturs (Picture © E. Hosseini)
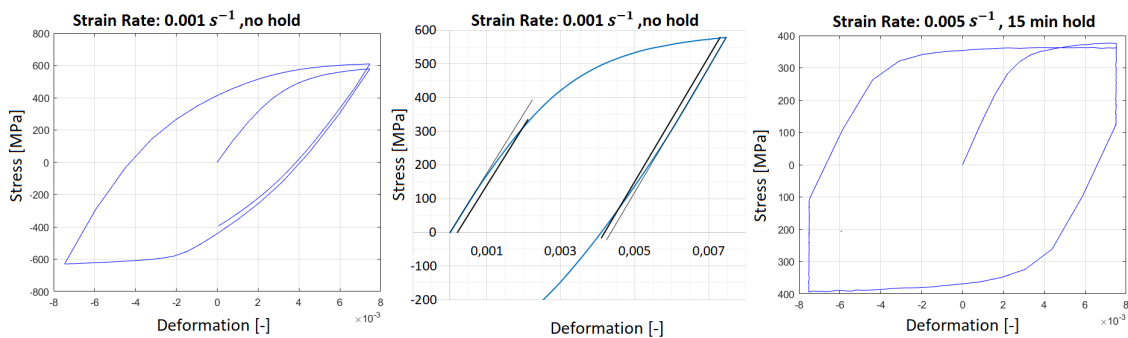
Figure 3.2: left: stress-strain response at $25°C$ without hold, center: same but with elastic extrapolation, right: stress-strain response at $800°C$ with hold

Looking at the results as pictures in Figure 3.2, we can observe some of the previously elaborated phenomena: In Test 16, after 1 cycle the stress at 0.75% is slightly higher than during the initial loading. This may indicate some elastic shakedown, which implies small amout of isotropic hardening. The Bauschinger effect is clearly visible: during the initial loading the specimen begins to yield at $\approx 150MPa$ and

during unloading it starts to yield at $\approx 275MPa$. The fact, the difference between the peak stress and the yield stress during the first compression is approximately twice as large as the initial yield stress indicates that little isotropic hardening is present. In Figure 3.2 right we observe that relaxation at $800°C$ is very prominent. This implies that creep is significant. Finally we clearly observe non-linear hardening as evidenced by a non-linear stress-strain relation in the plastic region.

4. Modeling calibrations

Figure 4.1: Flowchart of the fitting process

In this section we aim to fit our models to the experimental data described above. The whole process is illustrated in Figure 4.1: First we let MATLAB extract the time, strain, temperature and the stress information from experimental results. In order to reduce computational time, we fit the data to 100 logarithmically spread measurement points for each segment. The stresses and strains are linearly interpolated, if data is missing at this exact point in time.

Next, we define a series of variables $(x_1, \ldots, x_i)$, which will be used to derive the material properties as a function of temperature. How they relate is described below. The time and strain information, as well as our guessed material properties are passed on to Abaqus, which simulates the mechanical experiments of all test simultaneously. The results are extracted by MATLAB, which calculates the error between the simulated results and the experimental results. The optimisation toolbox will then systematically alter the input and rerun the simulation. The algorithm stops when the error becomes small enough. The full code is found in appendix A.

Chaboche

Elustic Deformation:

Elastic Deformation:	Young's Modulus:	$E = x_1[1 - x_2 \cdot \exp(T/x_3)]$
Plastic Deformation:	Tensile Stress:	$\sigma_y = x_4[1 - x_5 \cdot \exp(T/x_6)]$
		$C_1 = x_7[1 - x_9 \cdot \exp(T/x_{10})]$
		$C_2 = x_8[1 - x_9 \cdot \exp(T/x_{10})]$
		$\gamma_1 = x_{11}[1 - x_{13} \cdot \exp(T/x_{14})]$
		$\gamma_2 = x_{12}[1 - x_{13} \cdot \exp(T/x_{14})]$
		$Q_\infty = x_{19}[1 - x_{20} \cdot \exp(T/x_{21})]$
		$b = x_{22}[1 - x_{23} \cdot \exp(T/x_{24})]$
Creep:	Power Law Multiplier:	$A = x_{15}[x_{16}/(T + 273.14)^{x_{17}}]$
	Stress exponent:	$n = x_{18}$
	Time Order:	$m = 0$

Results:

Table 4.1: Fitted parameters of the Chaboche model with creep

E	$x_1 = 2.554 \cdot 10^6$	$x_2 = 9.307 \cdot 10^{-1}$	$x_3 = 5.868 \cdot 10^1$
σ_y	$x_4 = 2.572 \cdot 10^2$	$x_5 = 2.032 \cdot 10^{-2}$	$x_6 = 7.384 \cdot 10^3$
C	$x_7 = 2.575 \cdot 10^5$	$x_9 = 5.190 \cdot 10^{-1}$	$x_{10} = 1.997 \cdot 10^3$
	$x_8 = 1.952 \cdot 10^5$		
γ	$x_{11} = 4.905 \cdot 10^2$	$x_{13} = 5.313 \cdot 10^{-2}$	$x_{14} = 1.197 \cdot 10^4$
	$x_{12} = 1.289 \cdot 10^3$		
A	$x_{15} = 2.355 \cdot 10^1$	$x_{16} = 2.987 \cdot 10^2$	$x_{17} = 1.566 \cdot 10^{-1}$
n	$x_{18} = 6.370 \cdot 10^0$		
sum of squared errors:		$5.219 \cdot 10^{-1}$	

Table 4.2: Fitted parameters of the Chaboche model with isotropic hardening and creep

E	$x_1 = 2.004 \times 10^5$	$x_2 = 9.954 \times 10^{-2}$	$x_3 = 1.145 \times 10^3$
σ_y	$x_4 = 2.040 \times 10^2$	$x_5 = 6.557 \times 10^{-3}$	$x_6 = 2.572 \times 10^3$
C	$x_7 = 4.231 \times 10^5$	$x_9 = 4.563 \times 10^{-1}$	$x_{10} = 1.715 \times 10^3$
	$x_8 = 1.636 \times 10^4$		
γ	$x_{11} = 6.514 \times 10^2$	$x_{13} = 8.153 \times 10^{-3}$	$x_{14} = 7.129 \times 10^3$
	$x_{12} = 2.807 \times 10^2$		
Q_∞	$x_{19} = 5.837 \times 10^{-1}$	$x_{20} = 4.123 \times 10^{-2}$	$x_{21} = 1.75 \times 10^2$
b	$x_{22} = 1.005 \times 10^0$	$x_{23} = 7.015 \times 10^{-3}$	$x_{24} = 2.927 \times 10^7$
A	$x_{15} = 2.609 \times 10^1$	$x_{16} = 3.705 \times 10^2$	$x_{17} = 1.789 \times 10^{-1}$
n	$x_{18} = 6.450 \times 10^0$		
sum of squared errors:		4.18×10^{-1}	

Some observations from our results illustrated in Tables 4.1 and 4.2 and Figure 4.2: Q_∞ is very small throughout the observed temperature, as seen by $x_{19} = 5.837 \times 10^{-1} MPa$. This indicates that isotropic hardening plays small to no influence. Moreover, b, $s0$, g_1 and g_2 appear to be nearly independent of temperature as seen by $x_{24} \gg T_m$, $x_6 > T_m$ and $x_{14} > T_m$. Finally some of the material properties of chaboche and chaboche with isotropic hardening appear to be significantly different. However, the resulting stress-strain responses, as seen in Figure 4.3 and 4.4 change very little.
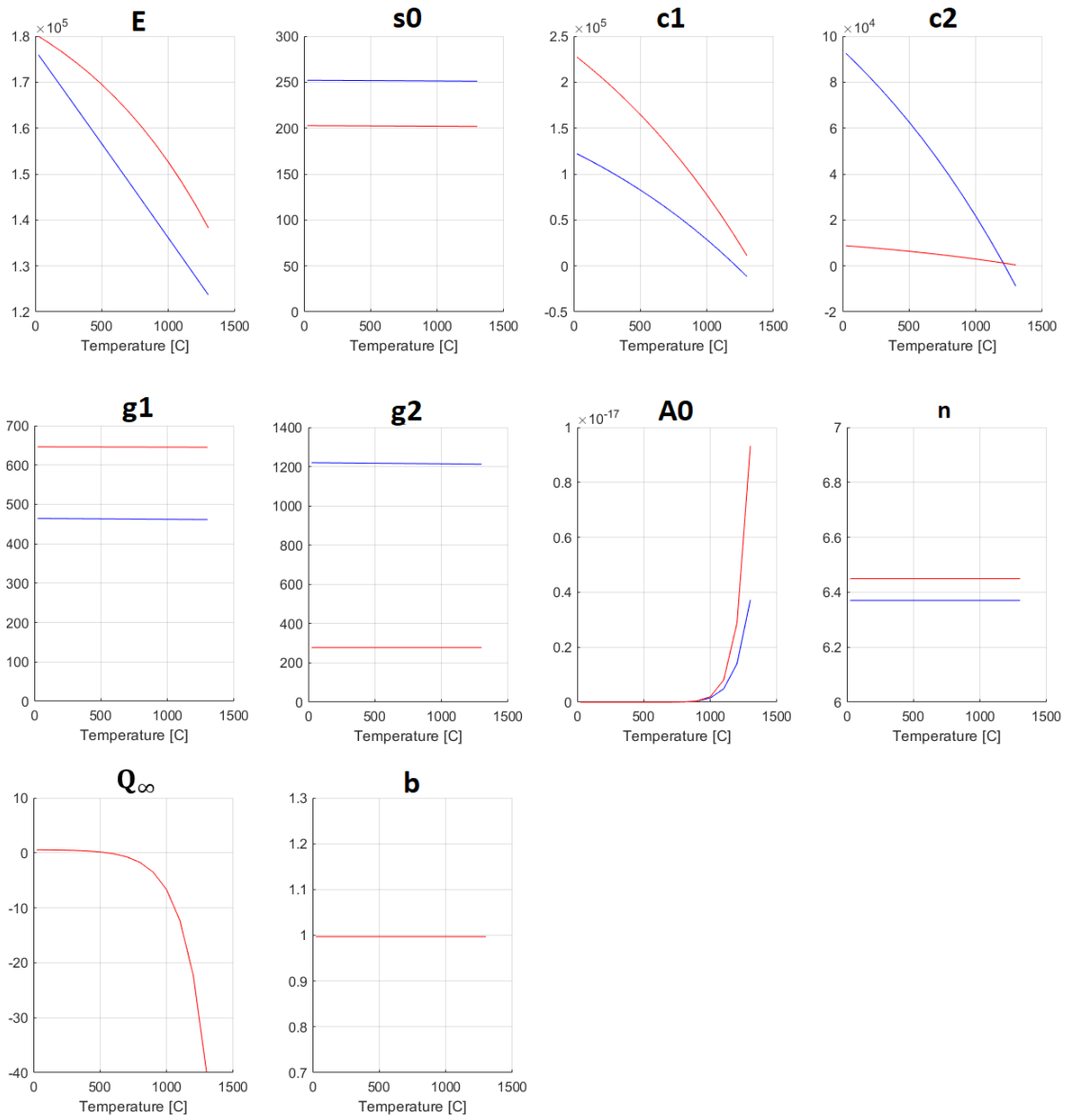
Figure 4.2: Plot of the material parameters (blue: chaboche, red: chaboche with isotropic hardening)
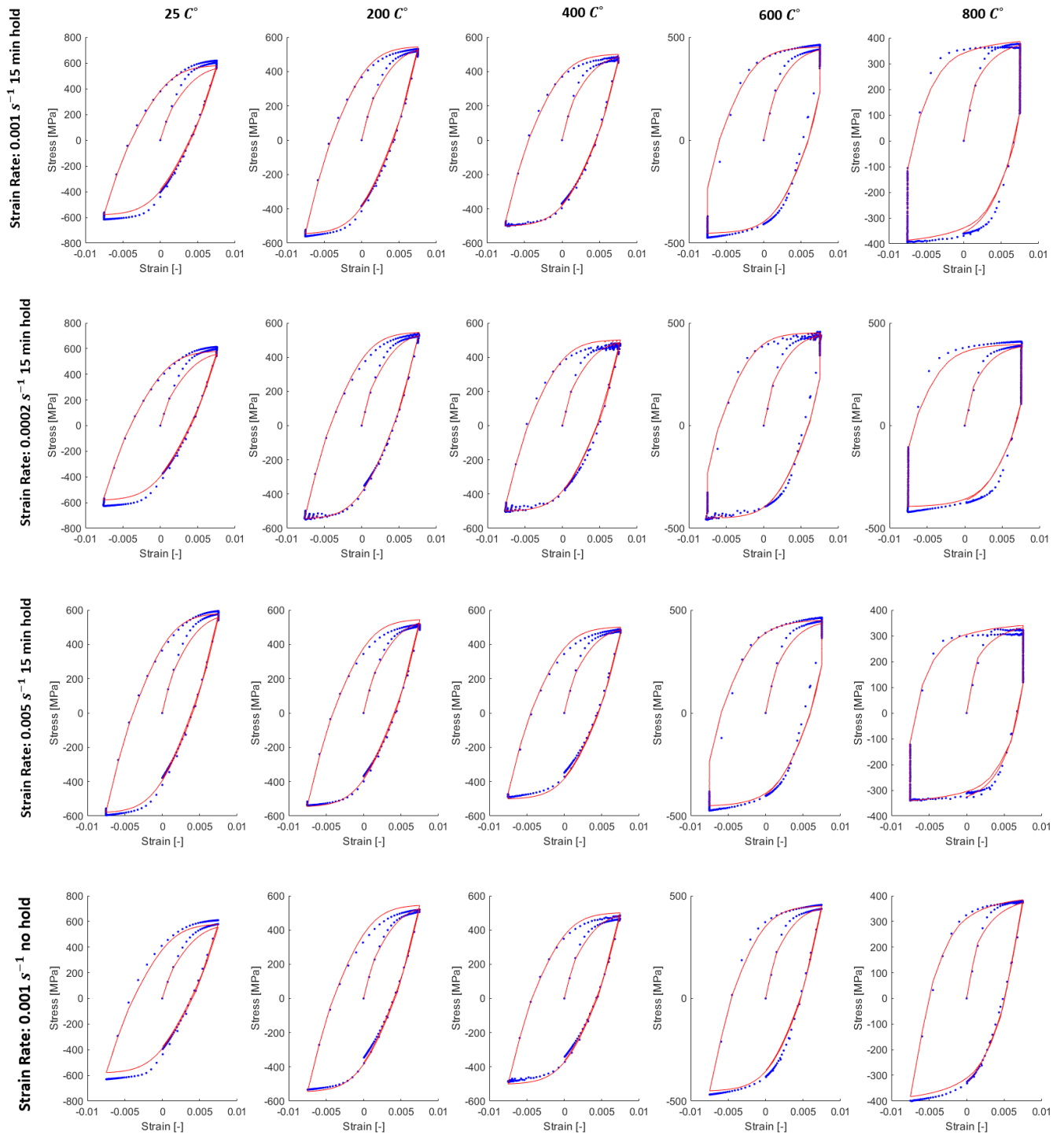
Figure 4.3: The test results for chaboche without the isotropic hardening (Blue: Experiment, Red: Model)
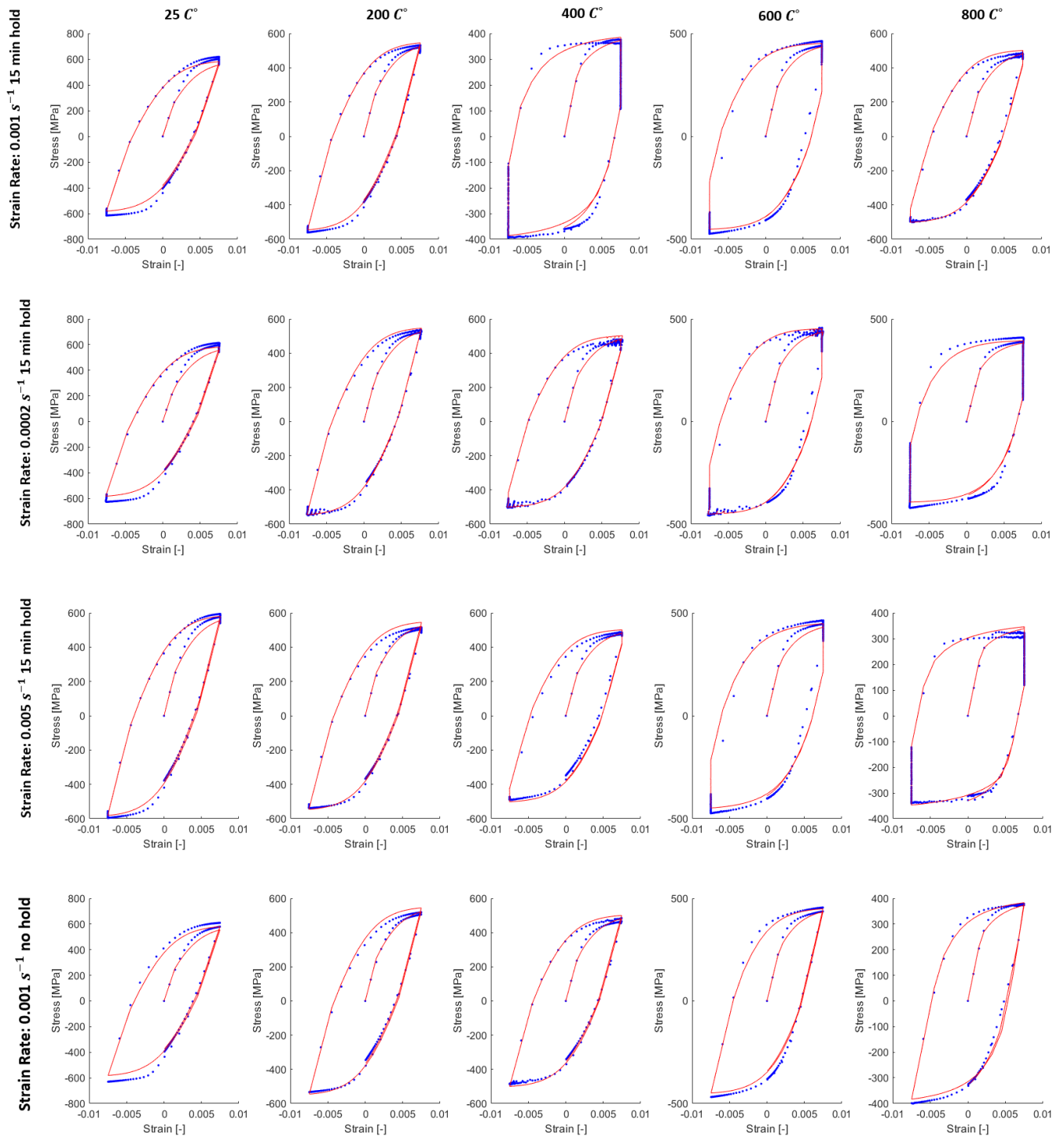
Figure 4.4: The test results for chaboche with the isotropic hardening (Blue: Experiment, Red: Model)

5. AM Simulation

Using the previously determined model parameters, we will simulate the manufacturing of a 2D Cantilever (Sketch in Figure 5.1). The reason we chose to simulate a 2D model is to reduce calculation time. The parameters used are listed in Table 5.1
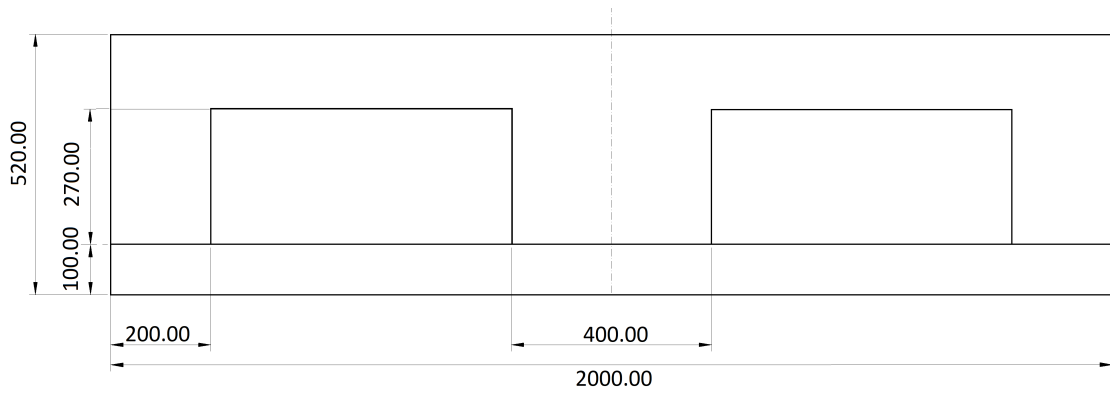
Figure 5.1: Dimensions of the simulated cantilever $[\mu m]$

Laser Power	$700W$
Scan Speed	$0.7m/s$
Layer Thickness	$30\mu m$
Laser Radius	$50\mu m$
Absorbtivity	0.2

Table 5.1: Settings for the additive manufacturing process

Conductivity 25$C°$	$9.1Wm^{-1}k^{-1}$
Conductivity 200$C°$	$14.1Wm^{-1}k^{-1}$
Conductivity 1300$C°$	$27.2Wm^{-1}k^{-1}$
Density	$8220kgm^{-3}$
Thermal expansion	$1.6 \times 10^{-5}K^{-1}$
Specific Heat 25$C°$	$486JKg^{-1}K^{-1}$
Specific Heat 1300$C°$	$858JKg^{-1}K^{-1}$

Table 5.2: Material Properties of Hastelloy X [11]

The layer size is $30\mu m$, which is slightly lower, than the industrial standard of $40 - 100\mu m$. [12] We will simulate the additive manufacturing process in ABAQUS. The reason for this choice is that ABAQUS allows the execution of user generated subroutines. This in turn allows us to simulate a moving heatsource, which melts and binds the powder, as well as program phase changes. It also allows us to model the phase transitions from powder to liquid, and back to solid by using field variables (See Fig 5.2). The full code is available in the appendix.
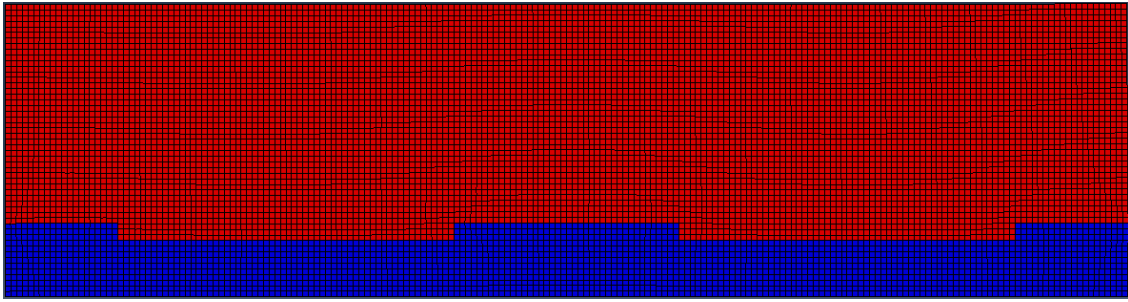
Figure 5.2: Field variables distribution after printing layer 1 (red: inactive elements, blue: active elements)

We can simulate the thermal component ahead of time and pass its results on to the mechanical simulation. The relevant data of the thermal component has been printed in Table 5.2. [11] The later adds the model parameters that we have determined previously, as well as our custom subroutine as written in the appendix. The results from these simulations will give us the residual stresses and distortion/deformation.

6. Results and Discussion

6.1 Thermal Results
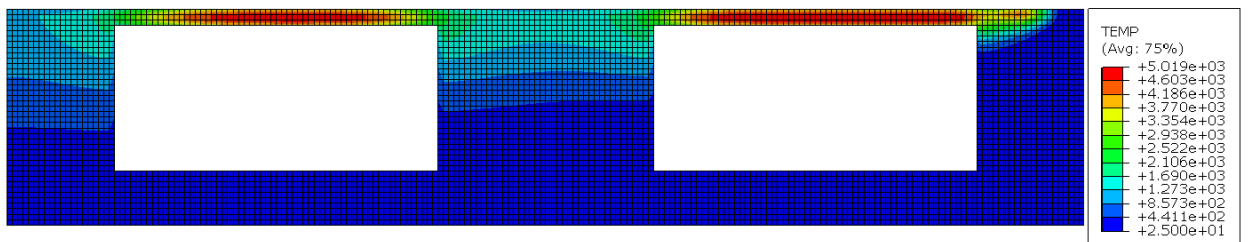
Figure 6.1: Temperature distribution while printing layer 10

Figure 6.1 shows how the temperatureat the overhang sections is much higher than near the supports. Reason being, that they can not conduct heat as easily to the substrate of the build. This means, that the temperature gradients near the corners is much higher than within the beam or the supports.

6.2 Mechanical Results
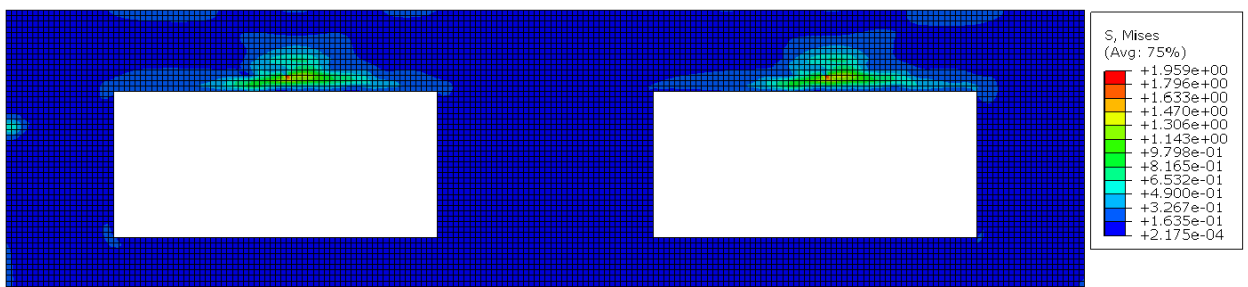
Figure 6.2: residual stress distribution if pure elasticity is assumed

Figure 6.2 shows the results if both plasticity and creep for Hastelloy X is ignored. As expected, no residual stresses are observed, as no plastic deformation can take place.
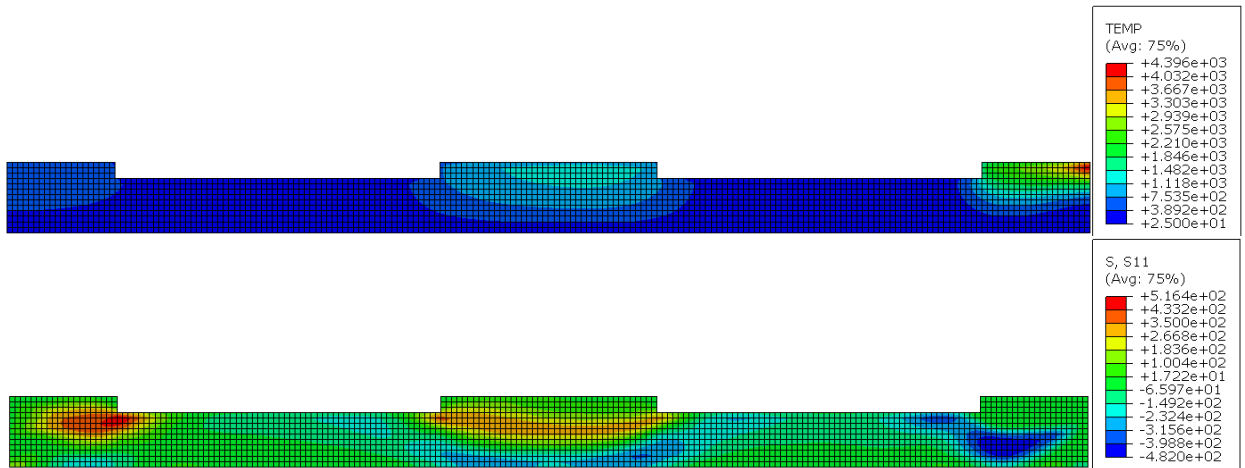
Figure 6.3: Process by which residual stresses are generated (top: Temperature, bottom: Stresses)

Thermal Stress: Figure 6.3 depicts the temperature and residual stress distriution during printing of layer 1. Here we can confirm the process by which residual stresses develop: On the right, while the laser passes over a specific section, the newest layers are stress free, due to unconstrained plastic flow. The layers below, which are still solid, experience compressive stresses, due to thermal expansion, while constrained. In the centre, where the laser has already passed, those previous layers are now beginning to compress, but are constrained by the layers at the bottom. This results in tensile stresses near the top and compressive stresses below.
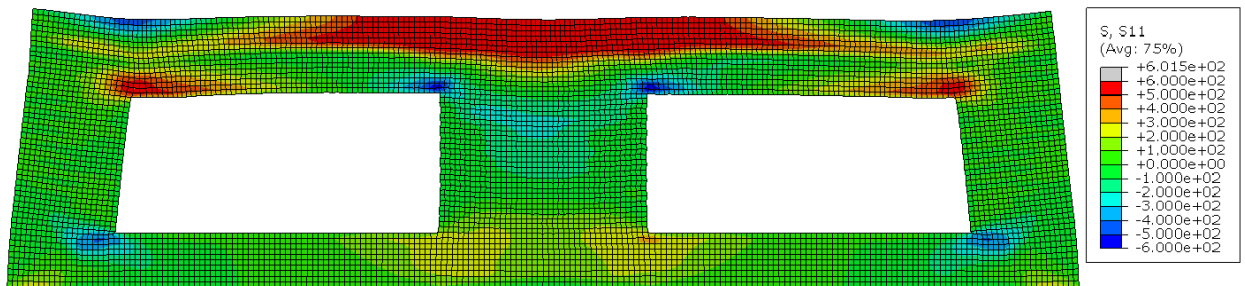
Figure 6.4: Residual stress distribution by concideration of Chaboche kinematic hardening without creep

Figure 6.4 depicts the residual stresses for a chaboche kinematic hardening model, while ignoring creep.

Location of Stress: We observe that the majority of stresses are in the top of our beam of our cantilever, while the bottom of the beam contains little to no stresses. This is in line to our expectations, as while printing, the bottom of the beam was unconstrained. This means that there was no force to counter the shrinkage of the

layer, resulting in the absence of residual stresses. Within the supports, there are few to no stresses. Reasoning being, that the subsequent layers will reheat the bottom ones, resulting in some relaxation of residual stress.

Magnidude of Stress: We observe that the stresses exceed 600 MPa, which is greater than the maximum amount of stress that we measured from our specimens in Chapter 3. This means, that we are extrapolating from our hardening model. This might be a good source of errors, unless the chosen model represent the material extremly well. Alternativly one could do tests at higher stresses. No residual stresses are observed within the supports, as they were reheated, allowing metal to deform and stresses to be reduced.

Stress concentration Additionally, stress concentrations exist near where the support structures meet the beam and the substrate. During printing, these are the locations, where the temperature gradient is also larger than in other parts, as the heat flow is greatest there.
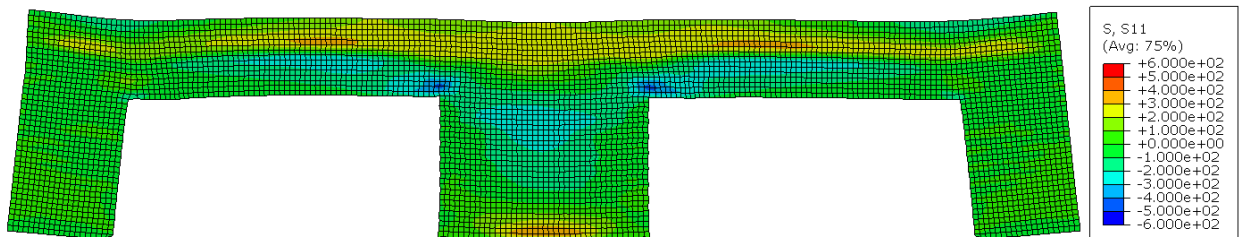
Figure 6.5: Residual stresses after removing the base plate

Deformation: Removing the base plate from the additively manufactured part reduces both the tensile and the compressive stresses at the top of the beam, and near the supports as seen in Figure 6.5. This implies however that some deformation has taken place. Looking at Figure 6.6 we observe that this is exactly what happened: The beam warps upward.
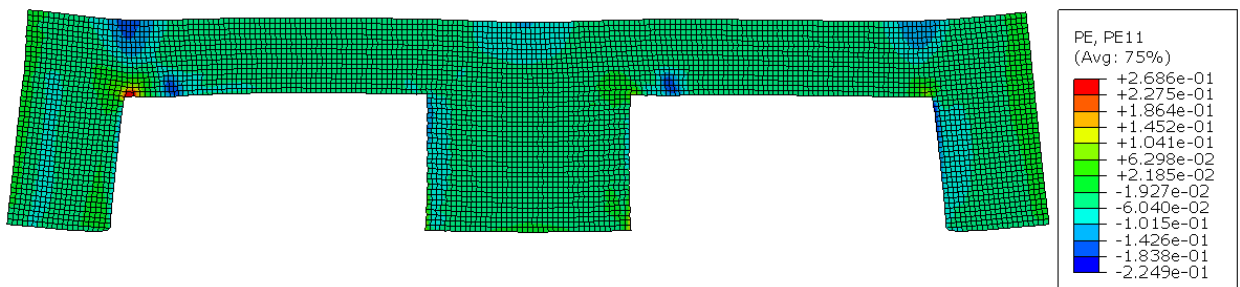
Figure 6.6: total deformation after release

Due to convergence issues, we are unable to present additional results and make comparisons. I can, however, offer some prediction how the results would have looked like: I assume that the inclusion of creep would result in lower residual stresses and subsequently smaller deformations. I expect only small difference if the isotropic part is added, since its contribution is minimal.

6.3   Summary and Outlook

The goal of this project is evaluating the sensitivity of predicted resudual streses within SLM pats to the type of considered constitutive model.

- confirm the theory which describes the origin of residual stresses that occur in additive manufacturing;

- pinpoint stress concentrations in an additively manufactured cantilever.

Convergance issues have precluded the comparison of different models, though.

A valuable extension for future research would be the simulation of a larger three-dimensional part. This would allow for the manufacturing of a part and subsequent validation of the model.

Bibliography

[1] M. Matsumoto, M. Shiomi, K. Osakada, and F. Abe, "Finite element analysis of single layer forming on metallic powder bed in rapid prototyping by selective laser processing," *International Journal of Machine Tools and Manufacture*, vol. 42, no. 1, pp. 61 – 67, 2002.

[2] A. Hussein, L. Hao, C. Yan, and R. Everson, "Finite element simulation of the temperature and stress fields in single layers built without-support in selective laser melting," *Materials and Design (1980-2015)*, vol. 52, pp. 638 – 647, 2013.

[3] Y.-L. Lee and M. E. Barkey, "Chapter 7 - fundamentals of cyclic plasticity theories," in *Metal Fatigue Analysis Handbook* (Y.-L. Lee, M. E. Barkey, and H.-T. Kang, eds.), pp. 253 – 297, Boston: Butterworth-Heinemann, 2012.

[4] Z. Zhuang, Z. Liu, and Y. Cui, "Chapter 2 - fundamental conventional concept of plasticity constitution," in *Dislocation Mechanism-Based Crystal Plasticity* (Z. Zhuang, Z. Liu, and Y. Cui, eds.), pp. 29 – 56, Academic Press, 2019.

[5] "Abaqus documentation: Isotropic elasto-plasticity." `https://classes.engineering.wustl.edu/2009/spring/mase5513/abaqus/docs/v6.5/books/stm/default.htm?startat=ch04s03ath104.html#stm-mat-isoelastoplast`.

[6] "Abaqus documentation: Models for metals subjected to cyclic loading." `https://classes.engineering.wustl.edu/2009/spring/mase5513/abaqus/docs/v6.5/books/usb/default.htm?startat=pt04ch11s02abm16.html`.

[7] G. B. Broggiato, F. Campana, and L. Cortese, "The chaboche nonlinear kinematic hardening model: calibration methodology and validation," *Meccanica*, vol. 43, pp. 115–124, Apr 2008.

[8] J. Chaboche, "Time-independent constitutive theories for cyclic plasticity," *International Journal of Plasticity*, vol. 2, no. 2, pp. 149 – 188, 1986.

[9] K. Naumenko and H. Altenbach, *Modeling of Creep for Structural Analysis*. 01 2007.

[10] "Abaqus documentation: Rate-dependent plasticity: creep and swelling." `https://classes.engineering.wustl.edu/2009/spring/mase5513/abaqus/docs/v6.6/books/usb/default.htm?startat=pt05ch18s02abm18.html`.

[11] "HASTELLOY X TECHNICAL DATA." `http://www.hightempmetals.com/techdata/hitempHastXdata.php`.

[12] T. Mukherjee, W. Zhang, and T. DebRoy, "An improved prediction of residual stresses and distortion in additive manufacturing," *Computational Materials Science,* vol. 126, pp. 360 – 372, 2017.

A. Code

The main_optimisation function dies the following:

1. extracts the deformations/stresses from our experiments

2. generates a set of starting variables from which the Material Parameters will be derived

3. optimises the Error_calculator_Hardening_KinematicOrIsotropic_Creep_No function

4. demands the plots for the final results

```
% This program optimises the parameters of a given constitutive model to be
% representative of a set of experimental data
clc
clear
close all
%% Importing experimental data from either excel or matlab database
if isfile('Experiment_Results.mat')
load 'Experiment_Results.mat'
else
for i=1:30
[num] = xlsread('Experiment_Results.xlsx',['Test_',num2str(i)]);
SegmentTime{i} = [num(1:101,1),num(1:101,5),num(1:101,9) ,num(1:101,13),
num(1:101,17),num(1:101,21),num(1:101,25)];
SegmenStrain{i} = [num(1:101,2),num(1:101,6),num(1:101,10),num(1:101,14),
num(1:101,18),num(1:101,22),num(1:101,26)];
SegmenTemp{i} = [num(1:101,3),num(1:101,7),num(1:101,11),num(1:101,15),
num(1:101,19),num(1:101,23),num(1:101,27)];
SegmenStress{i} = [num(1:101,4),num(1:101,8),num(1:101,12),num(1:101,16),
num(1:101,20),num(1:101,24),num(1:101,28)];
CompleteTest{i} = num(1:707,30:33);
SegmentField{i} = [num(1,34),num(1,35),num(1,36),num(1,37),num(1,38),
```

```
num(1,39),num(1,40)]/1000;
SegmentTime{i} = SegmentTime{i} ./ SegmentField{i};
clear num
end
clear i
save('Experiment_Results.mat')
end
%% Writing sections of abaqus input file
delete MatlabAbaqusInputs/*.txt
for i=1:30
for j=1:7
dlmwrite(['MatlabAbaqusInputs/Strain_amp_test_',num2str(i),'_Segment_',
num2str(j),'.txt'],[SegmentTime{i}(:,j),SegmenStrain{i}(:,j),],
'precision','%10.10f')
dlmwrite(['MatlabAbaqusInputs/Temp_amp_test_',num2str(i),'_Segment_',
num2str(j),'.txt'],[SegmentTime{i}(:,j),SegmenTemp{i}(:,j), ],
'precision','%10.10f')
%alternative for non natural field variables
dlmwrite(['MatlabAbaqusInputs/Field_Test_',num2str(i),'_Segment_',
num2str(j),'.txt'],['Test_',num2str(i),', ',
num2str(SegmentField{i}(1,j))],'delimiter','')
end
end
%% Start of optimization
% Material model parameters
Par0 =[1.7e+05,8.3e-02,4.0e+03,4.2e+02,3.8e-02,3.8e+02,8.0e+04,1.3e+04,2.3e-01,
6.9e+02,4.0e+02,4.6e+02,4.2e-02,3.6e+03,7.0e+03,2.6e+04,2e+00];
% initialising x vector
x0 = ones(size(Par0));
% fminsearch
fminsearch(@(x)Error_calculator_Hardening_KinematicOrIsotropic_Creep_No ...
(x,Par0,SegmenStress,CompleteTest,0),x0);
%% plotting
Error_calculator_Hardening_KinematicOrIsotropic_Creep_No ...
(x0,Par0,SegmenStress,CompleteTest,1)
```

The Error_calculator_Hardening_KinematicOrIsotropic_Creep_No does the following:

1. Takes the initial set of variables and modifies them

2. Derives the material parameters from the modified set of parameters and writes

them in .inp files

3. Calls ABAQUS and lets it run a simulation with the current set of material parameters

4. extracts the Stress/Strain results and compares them with the experimental results

5. returns an error back to main_optimisation.m

6. plots the final results

```
% Error_calculator_Hardening_KinematicOrIsotropic_Creep_No
% This program uses a set of model parameters and calculate the difference
% between the simulated and experimental stresses
function Error = Error_calculator_Hardening_KinematicOrIsotropic_Creep_No
(x,Par0,SegmenStress,CompleteTest,plotFLG)
Par=Par0.*abs(x);
dlmwrite('Model_Parameter_Error.txt',[0,Par],
'-append','precision','%10.10e')
% Defining a temperature vector
T = [25; 100; 200; 300; 400; 500; 600; 700; 800; 900; 1000; 1300];
sz_T=size(T);
% Calculate E, s0, c,g parameter (neccesary to generate _parameters.inp files)
E = Par(1)* (1-Par(2) .*exp(T./Par(3)));
s0 = Par(4)* (1-Par(5) .*exp(T./Par(6)));
c1 = Par(7)* (1-Par(9) .*exp(T./Par(10)));
c2 = Par(8)* (1-Par(9) .*exp(T./Par(10)));
g1 = Par(11)*(1-Par(13).*exp(T./Par(14)));
g2 = Par(12)*(1-Par(13).*exp(T./Par(14)));
%Plastic rate parameters
Q = Par(19)*(1-Par(20).*exp(T./Par(21)));
b = Par(22)*(1-Par(23).*exp(T./Par(24)));
%Pass on the field variable
Field = zeros(3*sz_T(1,1),1);
for i=1:sz_T(1,1)
Field(i+sz_T(1,1))= 1;
Field(i+2*sz_T(1,1))= 1000;
end
Temp=[T;T;T];
```

```matlab
A0 = [0*10.^Par(15)*exp(-(Par(16)./((T+273.14).^Par(17)))),10^-50);
max(1*10.^Par(15)*exp(-(Par(16)./((T+273.14).^Par(17)))),10^-50);
max(1000*10.^Par(15)*exp(-(Par(16)./((T+273.14).^Par(17)))),10^-50)];
m = [ones(size(T))*Par(18); ones(size(T))*Par(18); ones(size(T))*Par(18)];
n = [zeros(size(T)); zeros(size(T)); zeros(size(T))];
%% Writing material data for abaqus
delete MatlabAbaqusInputs/*.inp
dlmwrite('MatlabAbaqusInputs\Elastic_parameters.inp',
[E,0.34*ones(11,1),T],'precision','%10.10e')
dlmwrite('MatlabAbaqusInputs\Plastic_parameters.inp',
[s0,c1,g1,c2,g2,T],'precision','%10.10e')
dlmwrite('MatlabAbaqusInputs\Creep_parameters.inp',
[A0,m,n,Temp,Field],'precision','%10.10e')
%% Running ABAQUS
delete 'abaqus.*'
delete 'Model_result.*'
rmdir('Temp', 's')
mkdir Temp
system('abaqus job=Model_result input=Model.inp cpus=4 interactive ...
ask_delete=OFF scratch=Temp');
system('abaqus cae nogui=pythoncode.py');
%% If abaqus run is not successful
if or(~isfile('Model_result.rpt'),~isfile('Model_result.sta'))
Error = 1e7;
return
end
if findstring<1
Error = 1e7;
return
end
%% Reading simulation results and sampling
data = importdata('Model_result.rpt',' ');
data = data.data;
[x2,al,idx] = unique(data(:,1),'stable');
dataunique=data(al,:);
Sampling_1=(logspace(0,5,101)-1);
Sampling_1=Sampling_1/max(Sampling_1);
Sampling_2=sort(-Sampling_1+1);
Sampling_1=Sampling_1'*1000;
```

```
Sampling_2=Sampling_2'*1000;
Sampling= [Sampling_2;1e3+Sampling_1;2e3+Sampling_2;3e3+Sampling_1;
4e3+Sampling_2;5e3+Sampling_1;6e3+Sampling_2];
data_resample(:,1)=Sampling;
for i=1:30
data_resample(:,1+i)=interp1(dataunique(:,1),dataunique(:,1+i), ...
data_resample(:,1));
end
%% Error calculation
Error_seg_1(1:30)=0;
Error_seg_2(1:30)=0;
Error_seg_3(1:30)=0;
Error_seg_4(1:30)=0;
Error_seg_5(1:30)=0;
Error_seg_6(1:30)=0;
Error_seg_7(1:30)=0;
for i=1:30
Error_seg_1(i) = sum((SegmenStress{i}(:,1) - ...
data_resample( 1:101,1+i)).^2)/(sum(SegmenStress{i}(:,1).^2));
Error_seg_2(i) = sum((SegmenStress{i}(:,2) - ...
data_resample(102:202,1+i)).^2)/(sum(SegmenStress{i}(:,2).^2));
Error_seg_3(i) = sum((SegmenStress{i}(:,3) - ...
data_resample(203:303,1+i)).^2)/(sum(SegmenStress{i}(:,3).^2));
Error_seg_4(i) = sum((SegmenStress{i}(:,4) - ...
data_resample(304:404,1+i)).^2)/(sum(SegmenStress{i}(:,4).^2));
Error_seg_5(i) = sum((SegmenStress{i}(:,5) - ...
data_resample(405:505,1+i)).^2)/(sum(SegmenStress{i}(:,5).^2));
Error_seg_6(i) = sum((SegmenStress{i}(:,6) - ...
data_resample(506:606,1+i)).^2)/(sum(SegmenStress{i}(:,6).^2));
Error_seg_7(i) = sum((SegmenStress{i}(:,7) - ...
data_resample(607:707,1+i)).^2)/(sum(SegmenStress{i}(:,7).^2));
end
%% Error summation
Error = sum(Error_seg_1)+sum(Error_seg_2)+sum(Error_seg_3)+ ...
sum(Error_seg_4)+sum(Error_seg_5)+sum(Error_seg_6)+ ...
sum(Error_seg_7);
dlmwrite('Model_Parameter_Error.txt'[Error,sum(Error_seg_1), ...
sum(Error_seg_2),sum(Error_seg_3),sum(Error_seg_4), ...
sum(Error_seg_5),sum(Error_seg_6),sum(Error_seg_7)], ...
```

```
'-append','precision','%10.10e')
```

The subroutine contains two functions: DFLUX, which models the moving laser, and USDFLD which models phase transitions, and activates elements.

```fortran
C Subroutine for moving heat source modelling
SUBROUTINE DFLUX(FLUX,SOL,KSTEP,KINC,TIME,NOEL,NPT,COORDS,
1 JLTYP,TEMP,PRESS,SNAME)
INCLUDE 'ABA_PARAM.INC'
DIMENSION FLUX(2), TIME(2), COORDS(3)
CHARACTER*80 SNAME

C Variable declaration
REAL*8 x_coordinate,SCAN_SPEED,LASER_POWER,SUBST_HEIGHT,
1 LASER_RADIUS,ABSORPTIVITY,I0,x_laser_centre,
2 distance,LAYER_HEIGHT,PRINT_WIDTH,y_coordinate
C Rounding the coordinates
x_coordinate=IDNINT(COORDS(1)*1.D6)/1.D6
y_coordinate=IDNINT(COORDS(2)*1.D6)/1.D6

C Beam parameters
SCAN_SPEED = 700.D-3 ! Laser scan speed
LASER_POWER = 500.D-0 ! Laser power
LASER_RADIUS = 50.D-6 ! Laser radius
ABSORPTIVITY = 2.0D-1 ! Laser absorption coefficient

C Print parameters
PRINT_WIDTH = 100.D-6 ! Width of track
LAYER_HEIGHT = 30.0D-6 ! Layer thickness
C Substrate height
SUBST_HEIGHT = 100.0D-6 ! Hight of Substrate
C Initialy here is a vaccum above the substrate
IF ((y_coordinate .GT. SUBST_HEIGHT+ (KSTEP *LAYER_HEIGHT)) .OR.
1 (y_coordinate .LE. SUBST_HEIGHT+((KSTEP-1.D0)*LAYER_HEIGHT))
2 ) THEN
FLUX(1) = 0.D0
RETURN
END IF
```

```
C Turn laser off if between support/center
IF ((y_coordinate .LE. 3.7D-4)
1 .AND.(((x_coordinate.GT. 2.5D-4).AND.(x_coordinate .LT. 8.5D-4))
2 .OR. ((x_coordinate .GT.12.5D-4).AND.(x_coordinate .LT.18.5D-4))
3 )) THEN
FLUX(1) = 0.D0
RETURN
END IF
C Maximum flux intensity
I0 = ABSORPTIVITY*LASER_POWER/(2.D0*LASER_RADIUS*
1 PRINT_WIDTH*LAYER_HEIGHT)
C Coordinate of laser centre
x_laser_centre = TIME(1) * SCAN_SPEED

C Distance of node from laser center
distance = ABS(x_coordinate-X_LASER_CENTRE)

C Energy deposition
IF (distance .LE. LASER_RADIUS) THEN
FLUX(1) = I0*(1.D0-distance/LASER_RADIUS)
END IF
RETURN
END
C -----------------------------------------------
C Subroutine for material property assignments and element activation
SUBROUTINE USDFLD(FIELD,STATEV,PNEWDT,DIRECT,T,CELENT,
1 TIME,DTIME,CMNAME,ORNAME,NFIELD,NSTATV,NOEL,NPT,LAYER,
2 KSPT,KSTEP,KINC,NDI,NSHR,COORD,JMAC,JMATYP,MATLAYO,LACCFLA)
INCLUDE 'ABA_PARAM.INC'
CHARACTER*80 CMNAME,ORNAME
CHARACTER*3 FLGRAY(15)
DIMENSION FIELD(NFIELD),STATEV(NSTATV),DIRECT(3,3),
1 T(3,3),TIME(2)
DIMENSION ARRAY(15),JARRAY(15),JMAC(*),JMATYP(*),COORD(*)
C Variable declaration
REAL*8 x_coordinate,y_coordinate,temperature,LAYER_HEIGHT,T_MELT,
1 SUBST_HEIGHT

C Rounding the coordinates
```

```
x_coordinate=IDNINT(COORD(1)*1.D6)/1.D6
y_coordinate=IDNINT(COORD(2)*1.D6)/1.D6


C Layer height
LAYER_HEIGHT = 30.0D-6
C Substrate height
SUBST_HEIGHT = 100.0D-6


C Melting temperature
T_MELT = 1300.0D0


C No powder inbetween the supports/cantilever
IF ((y_coordinate .GT. SUBST_HEIGHT).AND.(y_coordinate .LT.3.7D-4)
1 .AND.(((x_coordinate.GT. 2.5D-4).AND.(x_coordinate .LT. 8.5D-4))
2 .OR. ((x_coordinate .GT.12.5D-4).AND.(x_coordinate .LT.18.5D-4))
3 )) THEN
FIELD(2)=1.D0
ELSE IF (y_coordinate .GT. SUBST_HEIGHT+(LAYER_HEIGHT*KSTEP)) THEN
FIELD(2)=1.D0
ELSE
FIELD(2)=0.D0
END IF



IF ((KSTEP .EQ. 1.D0 .AND. KINC .EQ. 1.D0).AND.
1 (y_coordinate .LE. SUBST_HEIGHT)) THEN
!Initialization of field variables at start of steps
! Substrate is solid
STATEV(1)= 2.D0
ELSE IF ((KSTEP .EQ. 1.D0 .AND. KINC .EQ. 1.D0).AND.
1 (y_coordinate .GT. SUBST_HEIGHT)) THEN
! Substrate is solid
STATEV(1)= 1.D0
ELSE IF ((KINC .EQ. 1.0D0).AND.
1 (y_coordinate .LE. SUBST_HEIGHT+(LAYER_HEIGHT*KSTEP)) .AND.
2 (y_coordinate .GT. SUBST_HEIGHT+(LAYER_HEIGHT*(KSTEP-1.0D0)))
3 )THEN
!At the beginning of each step a layer of powder is deposed
STATEV(1)=1.0D0
```

```fortran
      ELSE
!Reading temperature
CALL GETVRM ('TEMP ',ARRAY ,JARRAY ,FLGRAY ,JRCD ,JMAC ,JMATYP,
1 MATLAYO , LACCFLA )
temperature = ARRAY (1)
!Powder/solid to liquid transformation
IF (temperature .GT. T_MELT) THEN
STATEV(1) = 3.D0
END IF
!Liquid to solid to transformation
IF (STATEV(1).EQ.3.D0 .AND. temperature .LT. T_MELT) THEN
STATEV(1) = 2.D0
END IF
END IF
C Save the material state for next increment use
FIELD(1)=STATEV(1)
C Release at the end of calculations
IF ((y_coordinate .LT. SUBST_HEIGHT).AND.(KSTEP .EQ. 15.D0)) THEN
FIELD(2)=TIME(1)+DTIME
END IF
RETURN
END
```